International Journal of Information, Control and Computer Sciences
ISSN: 2517-9942
Vol:7, No:1, 2013

Image Clustering Framework for BAVM Segmentation in 3DRA Images: Performance Analysis

FH. Sarieddeen, R. El Berbari, S. Imad, J. Abdel Baki, M. Hamad, R. Blanc, A. Nakib, and Y. Chenoune

***Abstract*—**Brain ArterioVenous Malformation (BAVM) is an abnormal tangle of brain blood vessels where arteries shunt directly into veins with no intervening capillary bed which causes high pressure and hemorrhage risk. The success of treatment by embolization in interventional neuroradiology is highly dependent on the accuracy of the vessels visualization. In this paper the performance of clustering techniques on vessel segmentation from 3-D rotational angiography (3DRA) images is investigated and a new technique of segmentation is proposed. This method consists in: preprocessing step of image enhancement, then K-Means (KM), Fuzzy C-Means (FCM) and Expectation Maximization (EM) clustering are used to separate vessel pixels from background and artery pixels from vein pixels when possible. A post processing step of removing false-alarm components is applied before constructing a three-dimensional volume of the vessels. The proposed method was tested on six datasets along with a medical assessment of an expert. Obtained results showed encouraging segmentations.

***Keywords*—**Brain arteriovenous malformation (BAVM); 3-D rotational angiography (3DRA); K-Means (KM) clustering; Fuzzy C-Means (FCM) clustering; Expectation Maximization (EM) clustering; volume rendering.

I. Introduction

THE term “brain arteriovenous malformation” refers to a set of cerebral blood vessels comprising tangled abnormal vessels called the nidus, feeding arteries and draining veins [1]. Due to BAVMs, the blood directly flows from the arterial to the venous system without passing through the capillaries. This can cause an increasing in the veins pressure that can become extremely fragile and prone to bleeding. The most common BAVM symptoms include spontaneous hemorrhages, epileptic seizures, headaches, neurological deficits and progressive neurological deficits [2].

The gold standard for treatment of BAVMs is microsurgery, which was proved to be safe and effective for the majority of AVMs smaller than 3 cm in diameter [3]. Another approach is endovascular embolization that can be used alone or as a component of a multidisciplinary management [4]. BAVMs can also be treated via a radiosurgery [5] delivered by gamma knife, linear accelerator or heavy charged particle.

It is essential to precisely locate the position of vessels entering and leaving the malformation, as well as their radii and bending angles before treatment. Therefore many imaging techniques have been developed for this purpose. Conventional catheter angiography (CCA) is used at the end of follow-up to confirm complete occlusion [1], while for intermediate controls magnetic resonance angiography (MRA) with time of flight (TOF) or phase contrast techniques or computed tomography angiography (CTA) are usually used [6]-[8]. Digital subtraction angiography (DSA) with 3-D rotational angiography (3DRA) remains the standard technique [9], providing substantial additional information on BAVM angioarchitecture [10]-[11].

Despite the numerous different acquisition techniques, the neuroradiologists need a robust image processing techniques (vessel extraction, contrast enhancement, etc.) to be efficient during the intervention. Reviews on vessels extraction techniques [12]-[13] show that most techniques used in clinical purposes are semi-automatic requiring user intervention. Such techniques include specific geometric models problems [14], shape and flow driven methods [15], region growing and mathematical morphology [16]. One major problem for those methods is that they are not able to cope with the wide range of blood vessel pixel intensities. Weiler et al. [17] introduced a system (AVM-Explorer) for multi-volume visualization on vascular structures starting from MRI images. D. Babin et al. [18] proposed a segmentation algorithm based on projections in 3-D CTA images. M. Hernandez and A. Frangi [19] proposed an automatic method based on non-parametric geodesic active regions for segmentation of cerebrovascular structures with application to brain aneurysms in 3DRA and CTA images.

In the case of endovascular embolization treatment, the separation between the BAVM and the vessels is required in order to isolate the malformation. An automatic vessels' segmentation of 3DRA images is considered highly important and useful for the clinician, guiding him through the embolization process.

In this study, a framework that allows an automatic segmentation of the brain vessels from 3DRA images using different clustering methods is proposed. It allows extracting the vascular structures and the BAVMs from the background. The clustering algorithms: K-Means (KM), Fuzzy C-Means (FCM) and Expectation Maximization (EM) were separately tested and, the resulting outputs from each of the clustering algorithms where analyzed and compared. The rest of the paper

Sarieddeen H. is with FOE, Notre Dame University, Lebanon (hasarieddeen@ndu.edu.lb), El Berbari R. is with FOE, University of Balamand, Lebanon (racha.elberbari@balamand.edu.lb), Imad S. is with FOE, Notre Dame University, Lebanon (saimad@ndu.edu.lb), Abdel Baki J. is with FOE, Notre Dame University, Lebanon (jnabdelbaki@ndu.edu.lb), Hamad M. is with FOE, Notre Dame University, Lebanon (mhamad@ndu.edu.lb), Chenoune Y. is with PRIAM, ESME Sudria, Paris, France (chenoune@esme.fr), Blanc R. is with Fondation Ophtalmologique Adolphe de Rothschild, Paris, France (rblanc@fo-rothschild.fr), Nakib A. is with LISSI, Université Paris Est, France (amir.nakib@u-pec.fr).

is organized as follow: section II provides a detailed description of the methodology and the used clustering algorithms while section III presents the obtained results that are discussed in the last section before ending with a conclusion.

II. Materials

The 3DRA clinical datasets were acquired at the Interventional NeuroRadiology department at Fondation Ophtalmologique de Rothschild (Paris Franace) using a Philips Allura unit (Philips Healthcare, Netherlands). Rotational angiographies were performed using 28 cc of contrast agent, injected as 4cc per second with a delay of 3 second, and a 210-degree rotation. Each dataset was reconstructed on a 256 x 256 x 256 image with a voxel size of 0.496 x 0.496 x 0.496 mm^3

III. The Proposed Method

Fig. 1 shows the flowchart of the proposed framework for the automatic segmentation of brain vessels from 3DRA images. Each image is first processed alone and then the slices are combined into a 3-D image via volume rendering. The processing steps start by image enhancement followed by image clustering using one of the three different approaches (KM, FCM and EM). After the clustering step, a mask is created to remove unneeded components from the output image. Then each connected component of this output is treated separately for further cleaning.

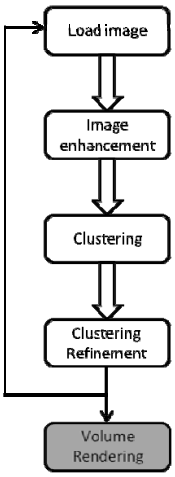

Fig. 1 Proposed framework flowchart

A. Image Enhancemet

A first preprocessing step of enhancement was needed in order to prepare the image for the clustering. Since the color intensity holds the needed information, nonlinear curves are avoided for contrast adjustment. Only the input range of the pixel intensities is clipped to focus on higher intensities.

B. Image Clustering

The goal of this step is to classify the pixels of the enhanced image into a given number of classes. We used 3 classes (clusters) for all our experiments. Below we present the different clustering techniques that we tested.

1. K-means (KM) Clustering

KM is an unsupervised statistical image segmentation algorithm that classifies the pixels into clusters based on their intensity values only without imposing special constraints. It is used because it is simple and has relatively low computational complexity. KM clustering is suitable for biomedical image segmentation because of the previously known number of clusters for images of particular regions of human anatomy [20]. However, KM is usually not sufficient when solely applied; hence it is either used in combination with other techniques such as watershed algorithm in [21] or optimized for image segmentation and made adaptive as in [22] or both as in [20].

KM algorithm classifies the input data points into multiple classes based on their inherent distance from each other. The points are clustered around the centroids that are obtained by minimizing the following objective function:

$$V = \sum_{i=1}^{k} \sum_{x_j \in S_i} (x_j - \mu_i)^2 \quad (1)$$

where there are k clusters S_i, $i = 1, 2 \ldots k$ and μ_i is the centroid or mean point of all the points (pixels) $x_j \in S_i$.

The algorithm [23] goes as follows: the intensity distribution (histogram) is first computed and k centroids with random intensities are initialized. The pixels are clustered based on the distance of their intensities from the centroid intensities and a new centroid for each of the clusters is then computed. This is repeated until the cluster labels of the image do not change anymore.

2. Fuzzy C-Means (FCM) Clustering

Like KM, FCM is an unsupervised clustering algorithm. However, unlike KM which is a hard segmentation algorithm, FCM is a type of soft segmentation that allows one piece of data to belong to two or more clusters at the same time [24]. FCM assigns pixels to each class by means of a fuzzy membership function. An image $X = (x_1, x_2, x_3 \ldots x_N)$ with N pixels can be categorized into C clusters by an iterative minimization of the following objective function [25]:

$$J = \sum_{j=1}^{N} \sum_{i=1}^{C} \mu_{ij}^{m} ||x_j - v_i||^2 \quad (2)$$

where μ_{ij} is the membership of pixel x_j in the i'th cluster, v_i is the i'th cluster center, m is the fuzzifier that controls the fuzziness of resulting partitions (any real number greater than 1) and $||.||$ is a norm metric. The membership function and cluster centers are updated as:

$$\mu_{ij} = \frac{1}{\sum_{k=1}^{c} \left(\frac{||x_j - v_i||}{||x_j - v_k||}\right)^{\frac{2}{m-1}}} \quad (3)$$

$$v_i = \frac{\sum_{j=1}^{N} \mu_{ij}^{m} x_j}{\sum_{j=1}^{N} \mu_{ij}^{m}} \quad (4)$$

This is repeated until $max_{ij}\left\{|\mu_{ij}^{(k+1)} - \mu_{ij}^{(k)}|\right\} < \varepsilon$, where ε is a termination criterion between 0 and 1, and k is the number of iteration steps.

Many image segmentation techniques were proposed using fuzzy clustering; these include Fuzzy Clustering with Spatial Probability, Fuzzy Logic Information C-Means Clustering Algorithm, Novel Fuzzy C-Means Clustering Algorithm and Improved Spatial Fuzzy C-Means Clustering Algorithm [26].

Besides, the application of FCM algorithm is explored as modified for MR brain tumor detection in [27], and with histogram based centroid initialization for brain tissue segmentation in MRI of head scans in [28].

3. Expectation Maximization (EM)

Expectation Maximization is one of the most common algorithms used for density estimation of data points in an unsupervised setting and it relies on finding the maximum likelihood estimates of parameters when the data model depends on certain latent variables [23],[29]. The EM algorithm consists of two steps: an expectation step, followed by a maximization step. The expectation is with respect to the parameters and conditions upon the observations while the maximization step provides a new estimate of parameters. The parameters found on the M step are used to begin another E step, and the process is repeated until convergence. EM is regularly used in image segmentation. It is combined with a Markov Random Field model for brain MR images in [28] and with distance measure for color image segmentation in [29].

C. Clustering Refinement

1. Filtering

The clustering result is not yet good enough; it showed to be still noisy, hence median filtering [30] is applied on the clustered image.

2. Masking

Even after filtering, some unwanted components remain in the image as shown in Fig. 2-d. A mask that would cover only the wanted components was needed. Such a mask is very helpful in this step as well as in the still to come cleaning step. Canny edge detection is used [31] to mark the boundaries of the image components. After obtaining the boundaries, they are filled up using basic morphological operations to result in a neat binary mask.

3. Cleaning

Since it is difficult to make the mask tight enough, one more refinement step was applied as follow: select each connected component in the mask, the mode of the pixels in the masked image under it is found and all pixels that have a different value from that mode value are set to zero.

D. Volume Rendering

Finally, a 3-D volume is constructed from the processed slices. Shear-warp colored volume rendering [32] with bilinear interpolation is used with the color map jet.

IV. Results

In the following, the obtained results for each step of the process are presented.

The best image enhancement results for each clustering algorithm clipped the input range into: [0.357±0.077 , 0.881±0.184] for KM, [0.357±0.077 , 1±0] for FCM and [0.34±0.09 , 0.983±0.04] for EM. The range of [0.325, 1] was applied on all cases. An enhanced image for the case of KM clustering is shown in Fig. 2-b.

At the clustering step, the number of clusters was set to 3 aiming at segmenting arteries from veins and from background. However, the image intensity did not carry enough information for such segmentation and clear distinction between arteries and veins was not achieved. Fig. 2-c shows the output after KM clustering. The outputs from each of the tested clustering algorithms were almost identical as shown in Fig. 3 when compared to Fig. 2-c. However, KM had the best convergence time followed by EM and FCM.

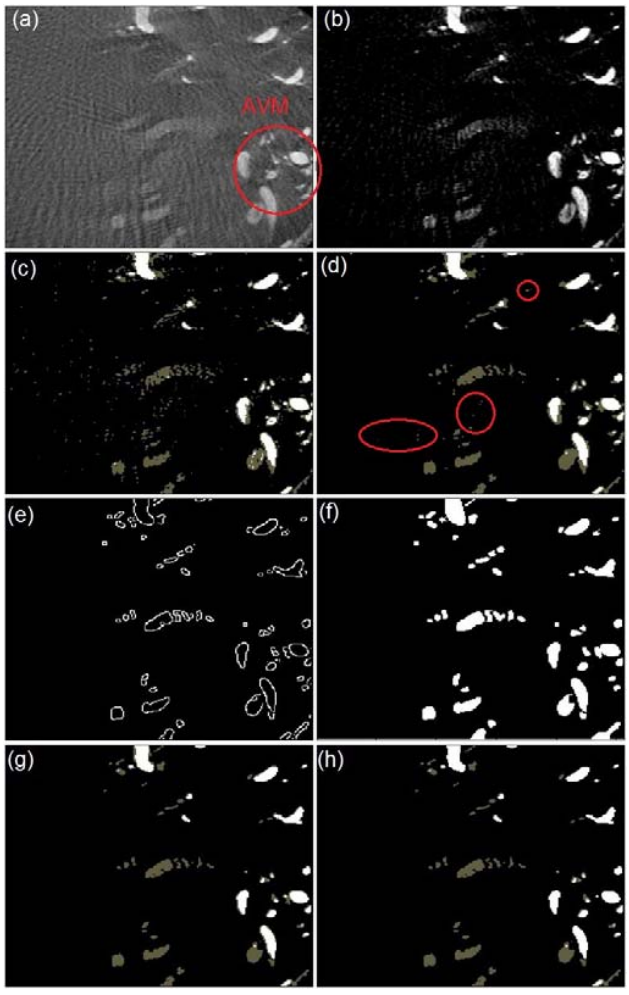

Fig. 2 (a) The original image showing AVM, (b) Contrast enhancement, (c) Resulting image after KM clustering, (d) Filtered clustered output showing small, unwanted component to be masked, (e) Edge detection, (f) Filled mask, (g) Masked output and (h) Cleaned output

Median filtering proved its importance in reducing the number of wrongly classified pixels (Fig. 2-d). It also helped in preparing a neat mask to be used next on the clustered image. The Canny sensitivity threshold is set empirically to 0.155. Fig. 2-e shows the output after the edge detection step.

Hence, a neat mask is obtained as shown in Fig. 2-f. All components in the filtered image that did not fall under the components of the mask were erased to obtain a masked output as shown in Fig. 2-g.

To avoid the loss of information due to the cleaning process, some constraints were added such as limiting this operation to components greater than a specific size and skipping it if the majority of pixels under the mask component are black. The cleaned output is shown in Fig. 2-h.

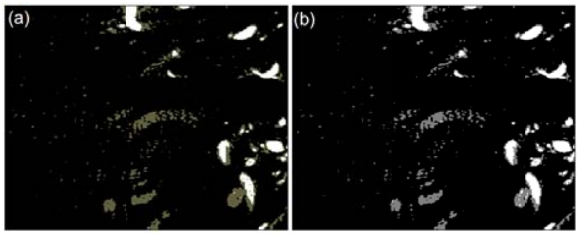

Fig. 3 (a) The resulting image after FCM clustering and (b) after EM clustering

Finally, upon volume rendering and after segmenting into 3 clusters, most vessels appeared in red and some segments appeared in blue, distributed, sometimes, within red segments (Fig. 4-a). BAVMs were clearly identified in some cases as shown in Fig. 4-f.

V. Discussion and Conclusion

In this paper, a framework to segment brain vessels from 3DRA images was proposed.

Three different clustering algorithms; KM, FCM and EM were tested and compared. Almost identical clustering results were obtained with the three algorithms. K-Mean was used in the rest of this study, as it had the shortest convergence time when compared to EM and FCM.

Clustering results were refined in post-processing step in order to reduce the number of wrongly classified pixels.

Finally, satisfying three dimensional reconstructions of the vessels from the obtained 2D segmentations were obtained.

In the proposed framework, the image pixels intensity was the only information used to carry out the segmentation process.

However, it is known that the intensity of the vascular structures depends on the presence of the contrast medium besides the vessel where the medium was injected (carotid or vertebral). High flow shunts and large size of AVMs have impacts on the contrast medium dilution in the blood and thus can influence the gray level intensity of the images.

Moreover, in datasets acquired under low contrast dose, strong image artifacts are visible within the same range of intensities of vessels. Fig. 4-a is an example of such a case where blue segments appear within red ones due to bone shadow.

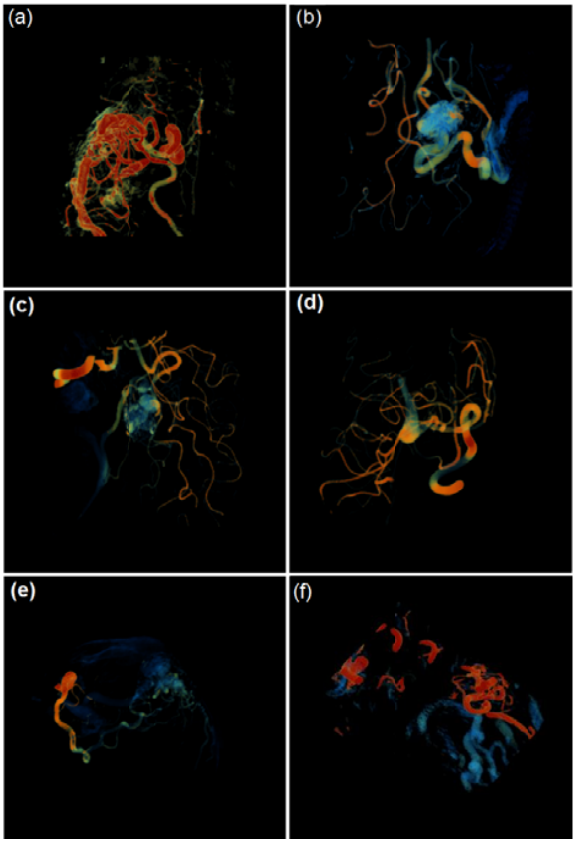

Fig. 4 The 3D final outputs of the six processed datasets using KM clustering after an enhancement that clipped the input range into [0.325 1]

All the three dimensional outputs in Fig. 4 were obtained with the same set of parameters. The developed method is hence suitable for the segmentation of the whole injected vessels without requiring any user intervention.

In the obtained results, vessels were segmented from the background and within these vessels; the blue color indicates a low density of contrast medium.

The main issue in segmenting 3DRA images is faced when the same tissue can correspond to different intensity ranges depending on the imaging device, settings and contrast injection protocol.

Besides, another limitation is related to the fact that BAVMs could be fed by several arteries that might not be injected by the contrast media at the same time.

All these limitations make the task of automatically separating arteries from veins on the 3DRA images, by using the gray intensities as unique criterion for the segmentation very difficult.

In order to facilitate the vessels separation task, the segmentation process should rely on anatomical knowledge, to be introduced in the image. This anatomical knowledge could be expressed by using a reference set, segmented and marked

manually by the clinician in order to support the automatic process, by identifying critical points or paths.

On the other hand, image intensity standardization [33] could also be combined to this anatomical knowledge for better segmentation results on 3DRA images.

In work under progress, the proposed approch is to be combined with an anatomical knowledge reference that is currently under preparation, to achieve better results concerning the separation of arteries and veins.

REFERENCES

[1] J. Byrne, "Cerebrovascular malformations," Eur. Radiol., 15: 448–452, 2005.

[2] H. Mast, JP. Mohr, A. Osipov, J. Pile-Spellman, RS. Marshall, RM. Lazar, BM. Stein, WL. Young, "'Steal' is an unestablished mechanism for the clinical presentation of cerebral ateriovenous malformations," Stroke 26: 1215–1220, 1995.

[3] J. Pik J, MK. Morgan, "Microsurgery for small arteriovenous malformations of the brain: Results of 110 consecutive cases," Neurosurgery, 47: 571-577, 2000.

[4] YP. Gobin, A. Laurent, L. Merienne, et al, "Treatment of brain arteriovenous malformations by embolization and radiosurgery," J Neurosurg 85: 19–28, 1996.

[5] M. Schlienger, D. Atlan, D. Lefkopoulos, et al, "Linac radiosurgery for cerebral arteriovenous malformations: results in 169 patients," Int J Radiat Oncol Biol Phys 46: 1135–42, 2000.

[6] JY Gauvrit, C. Oppenheim, F. Nataf, et al, "Three-dimensional dynamic magnetic resonance angiography for the evaluation of radiosurgically treated cerebral arteriovenous malformations," Eur Radiol 16: 583–591, 2006.

[7] L. Remonda, P. Senn, A. Barth, M. Arnold, KO. Lovblad, G. Schroth, "Contrast-enhanced 3D MR angiography of the carotid artery: comparison with conventional digital subtraction angiography," Am J Neuroradiol 23: 213–219, 2002.

[8] PC. Sanelli, MJ. Mifsud, PE. Stieg, "Role of CT angiography in guiding management decisions of newly diagnosed and residual arteriovenous malformations," Am J Roentgenol 183: 1123–1126, 2004.

[9] RM. Friedlander, "Arteriovenous malformations of the brain," New England Journal of Medicine, 356(26): 2704-2712, 2007.

[10] C. Cavedon, "Three-dimensional rotational angiography (3DRA) adds substatial information to radiosurgery treatment planning of AVM's compared to angio-CT and angio-MR," Med Phys 31(8): 2181–2, 2004.

[11] X. Combaz, O. Levrier, J. Moritz, J. Mancini, JM. Regis, JM. Bartoli, NJ. Girard, "Three-dimensional rotational angiography in the assessment of the angioarchitecture of brain arteriovenous malformations," Neuroradiol. 38(3): 167-74, 2011.

[12] Z. Yaniv, K. Cleary, "Computer Aided Interventions and Medical Robotics, Image-guided procedures: A review,", Image Science and Information Systems Center, Georgetown University Medical Center, Washington, DC, Tech. Rep., 2006.

[13] D. Lesage, E.D. Angelini, I. Bloch, G. Funka-Lea, "A review of 3D Vessel Lumen Segmentation Techniques: Models, Features and Extraction Schemes," Medical Image Analysis 13(6): 819-845, 2009.

[14] M. Piccinelli, A. Veneziani, D.A. Steinman, A. Remuzzi, L. Antiga, "A Framework for Geometric Analysis of Vascular Structures: application to Cerebral Aneurysms," IEEE Transactions on Medical Imaging, 1141-1155, 2009.

[15] D. Nain, A. Yezzi, G. Turk, "Vessel segmentation using a shape driven flow," Intl. Conf. on Medical Image Computing and Comp. Ass. Intervention (MICCAI), 51–59, 2003.

[16] M. Donizelli, "Region-oriented segmentation of vascular structures from dsa images using mathematical morphology and binary region growing", Bildverarbeitung für die Medizin, 12: *CEUR Workshop proceeding*, 1998

[17] *F. Weiler, C. Rieder, C. A. Da*vid, C. Wald, and H. K. Hahn, "Avm-explorer: Multi-volume visualization of vascular structures for planning of cerebral avm surgery," Eurographics Association, Llandudno, UK, 9-12, 2011.

[18] D. Babin, E. Vansteenkiste, A. Pizurica and W. Philips, "Segmentation of brain blood vessels using projections in 3-D CT angiography images," IEEE EMBS, 8475–8478, 2011.

[19] M. Hernandez, AF. Frangi, "Non-parametric geodesic active regions: method and evaluation for cerebral aneurysms segmentation in 3DRA and CTA," Med Image Anal 11: 224–241, 2007.

[20] C.W. Chen, J. Luo, K.J. Parker, "Image segmentation via adaptive K-mean clustering and knowledge based morphological operations with biomedical applications", IEEE Transactions on Image Processing, 7(12): 1673-1683, 1998.

[21] H. Ng, S. Ong, K. Foong, P. Goh, and W. Nowinski, "Image segmentation using k-means clustering and improved watershed algorithm," IEEE Southwest Symp. Image Anal. Interpretation, 61– 65, 2006.

[22] A. S. Binsamma and R. AbdulSalam, "Adaptation of K Means Algorithm for Image Segmentation," International Journal of Signal Processing, 5(4): 270–274, 2009.

[23] S. Tatiraju and A. Mehta, "Image segmentation using k-means clustering, EM and normalized cuts," UC Irvine, 2008.

[24] B.Sathya, R.Manavalan, "Image Segmentation by Clustering Methods: Performance Analysis," International Journal of Computer Applications, 29(11): 0975 – 8887, 2011.

[25] M.C.J. Christ and R.M.S. Parvathi, "Fuzzy c-means algorithm for medical image segmentation," Electronics Computer Technology (ICECT), 2011 3rd International Conference on , 4: 33-36, 2011.

[26] S. Naz, H. Majeed, H. Irshad, "Image segmentation using fuzzy clustering: A survey," Emerging Technologies (ICET), 6th International Conference 181-186, 2010.

[27] M. Shasidhar, V.S. Raja, B.V. Kumar, "MRI Brain Image Segmentation Using Modified Fuzzy C-Means Clustering Algorithm," Communication Systems and Network Technologies (CSNT), International Conference, 473-478, 2011.

[28] T. Kalaiselvi, K. Somasundaram, "Fuzzy c-means technique with histogram based centroid initialization for brain tissue segmentation in MRI of head scans," Humanities, Science & Engineering Research (SHUSER), 2011 International Symposium, 149-154, 2011.

[29] T.K. Moon, "The expectation-maximization algorithm," Signal Processing Magazine, IEEE , 13(6): 47-60, 1996.

[30] Y. Zhang, M. Brady and S. Smith, "Segmentation of brain MR images through a hidden Markov random field model and the expectation-maximization algorithm," IEEE Transactions on Medical Imaging, 20(1): 45-57, 2001.

[31] M.S. Nair, R. Rajasree, J. John, and M. Wilscy , "Expectation-Maximization with Distance Measure for Color Image Segmentation," IEEE Region 10 and the Third international Conference on Industrial and Information Systems, 1-5, 2008.

[32] R. H. Chan, C. Ho, M. Nikolova, "Salt-and-Pepper Noise Removal by Median-type Noise Detectors and Detailpreserving Regularization," IEEE Transactions on Image Processing, 14: 1479–1485, 2005.

[33] L. Ding, A. Goshtasby, "On the Canny edge detector", Pattern Recognition, 34: 721-725, 2001.

[34] P. Lacroute, "Analysis of a parallel volume rendering system based on the shear-warp factorization," IEEE Transactions on Visualization and Computer Graphics, 2(3): 218– 231, 1996.

[35] H. Bogunovic, A. G. Radaelli, M. D. Craene, D. Delgado, and A. F. Frangi, "Image intensity standardization in 3d rotational angiography and its application to vascular segmentation," Proc. SPIE Med. Imag., 6914: 91419–91419, 2008.